Comprehensive phenotyping of erythropoiesis in human bone marrow: Evaluation of normal and ineffective erythropoiesis

Hongxia Yan, Abdullah Ali, Lionel Blanc, Anupama Narla, Joseph Lane, Erjing Gao, Julien Papoin, John Hale, Christopher Hillyer, Naomi Taylor, et al.

HHS Public Access

Author manuscript

Am J Hematol. Author manuscript; available in PMC 2022 September 01.

Published in final edited form as:

Am J Hematol. 2021 September 01; 96(9): 1064–1076. doi:10.1002/ajh.26247.

Comprehensive phenotyping of erythropoiesis in human bone marrow: Evaluation of normal and ineffective erythropoiesis

Hongxia Yan, MS[1], **Abdullah Ali, PhD**[2], **Lionel Blanc, PhD**[3,4], **Anupama Narla, MD**[5], **Joseph M Lane, MD**[6,7], **Erjing Gao, BS**[1], **Julien Papoin, MS**[3], **John Hale, PhD**[1], **Christopher D Hillyer, MD**[1], **Naomi Taylor, MD, PhD**[8,9], **Patrick G. Gallagher, MD**[10,11,12], **Azra Raza, MD**[2], **Sandrina Kinet, PhD**[8,*], **Narla Mohandas, DSc**[1,*]

[1]New York Blood Center, New York, NY, USA;

[2]Myelodysplastic Syndromes Center, Columbia University NY, USA;

[3]The Feinstein Institute for Medical Research, Manhasset, NY, USA;

[4]Zucker School of Medicine at Hofstra/Northwell, Hempstead, NY, USA;

[5]Stanford University School of Medicine, Stanford, CA, USA;

[6]Department of Orthopaedic Surgery, Hospital for Special Surgery, New York, NY, USA;

[7]Department of Orthopaedic Surgery, NewYork-Presbyterian Hospital, Weill Cornell Medical Center, New York, NY, USA;

[8]Institut de Génétique Moléculaire de Montpellier, University of Montpellier, CNRS, Montpellier, France;

[9]Pediatric Oncology Branch, NCI, CCR, NIH, Bethesda, MD, USA;

[10]Department of Pediatrics, Yale University School of Medicine, New Haven, CT, USA

[11]Department of Pathology, Yale University School of Medicine, New Haven, CT, USA

[12]Department of Genetics, Yale University School of Medicine, New Haven, CT, USA

Abstract

Identification of stage-specific erythroid cells is critical for studies of normal and disordered human erythropoiesis. While immunophenotypic strategies have previously been developed to identify cells at each stage of terminal erythroid differentiation, erythroid progenitors are currently defined very broadly. Refined strategies to identify and characterize BFU-E and

Correspondence: Narla Mohandas D.Sc., New York Blood Center, 310 E67th street, New York, NY, USA; Tel: (212)-570-3056, fax: (212)-570-3264, MNarla@nybc.org.

Authorship

H.Y and N.M designed the research; H.Y and E.G performed most of the experiments; H.Y., A. A., L.B., A.N., J.M.L, J.P., J.H., C.D.H., N.T., P.G.G., A.R., S.K., and N.M. analyzed and interpreted the data; H.Y. and N.M. cowrote the manuscript; A.A., L.B., A.N., C.D.H., N.T., P.G.G., and S.K. edited the manuscript; and all authors read and commented on the final manuscript.

*Co-senior authors

Conflict of interests

None.

Data Availability Statement

The data that support the findings of this study are available from the corresponding author upon reasonable request.

CFU-E subsets are critically needed. To address this unmet need, a flow cytometry-based technique was developed that combines the established surface markers CD34 and CD36 with CD117, CD71, and CD105. This combination allowed for the separation of erythroid progenitor cells into 4 discrete populations along a continuum of progressive maturation, with increasing cell size and decreasing nuclear/cytoplasmic ratio, proliferative capacity and stem cell factor responsiveness. This strategy was validated in uncultured, primary erythroid cells isolated from bone marrow of healthy individuals. Functional colony assays of these progenitor populations revealed enrichment of BFU-E only in the earliest population, transitioning to cells yielding BFU-E and CFU-E, then CFU-E only. Utilizing CD34/CD105 and GPA/CD105 profiles, all 4 progenitor stages and all 5 stages of terminal erythroid differentiation could be identified. Applying this immunophenotyping strategy to primary bone marrow cells from patients with myelodysplastic syndrome, identified defects in erythroid progenitors and in terminal erythroid differentiation. This novel immunophenotyping technique will be a valuable tool for studies of normal and perturbed human erythropoiesis. It will allow for the discovery of stage-specific molecular and functional insights into normal erythropoiesis as well as for identification and characterization of stage-specific defects in inherited and acquired disorders of erythropoiesis.

INTRODUCTION

The human bone marrow generates ~2.5 million red cells every second at steady state through a process defined as erythropoiesis[1]. In contrast to the myeloid and lymphoid lineages where high throughput immunophenotyping has allowed for the characterization of distinct development stages[2–4], it is still not possible to comprehensively phenotype all distinct stages of erythropoiesis. This is an area of particular relevance in cases of ineffective erythropoiesis where disturbances in the normal progression of erythroid differentiation contributes to anemia (e.g., thalassemia, Diamond-Blackfan anemia and myelodysplastic syndromes (MDS)).

Since the development of single parameter flow cytometry analysis in the 1980s[5,6], there has been progress in defining cell surface markers that allow for the identification of human erythroid progenitors and terminally differentiating erythroblasts[7–16]. Using Glycophorin A (GPA), α4-integrin and Band 3 as surface markers, we were previously able to resolve and quantify five distinct stages of terminally differentiating erythroblasts[12]. Furthermore, four different surface markers have been used to identify BFU-E as $IL3R^{-}GPA^{-}CD34^{+}CD36^{-}$ and CFU-E as $IL3R^{-}GPA^{-}CD34^{-}CD36^{+}$ [14]. In addition, a transient population of $IL3R^{-}GPA^{-}CD34^{+}CD36^{+}$ progenitor cells were identified in an *in vitro* model of adult erythropoiesis[17]. However, these latter markers do not allow homogeneous subsets to be distinguished[18]; BFU-E and CFU-E progenitor populations that are defined in this manner are functionally heterogeneous, as reflected in their generation of colonies of markedly different sizes(our unpublished data).

Here, we aimed to resolve the heterogeneity of these early stages of erythropoiesis. By combining established surface markers (CD34 and CD36) with CD117 (c-kit), CD71 and CD105, we were able to isolate four distinct erythroid progenitor populations and resolve the continuum of early erythropoiesis. Furthermore, our studies reveal that the

expression kinetics of CD105 allow the previously identified five stages of terminal erythroid differentiation to be distinguished.

Based on our previous and current data, we were able to use a 10-color flow cytometry panel to quantitate nine distinct erythroid stages in normal human bone marrow. To evaluate the relevance of these findings in diseases with disordered erythropoiesis, we tested this novel flow cytometry panel in a small cohort of patients with myelodysplastic syndromes (MDS). We observed that ineffective erythropoiesis in MDS patients is associated with stage-specific erythroid defects. Thus, our novel and comprehensive strategy for the phenotyping of human bone marrow erythropoiesis reveals novel aspects of the continuum in normal and disordered human erythropoiesis.

MATERIALS AND METHODS

Sources of CD34$^+$ cells and primary human bone marrow samples

Leukopaks were obtained from the New York Blood Center. Bone marrow tissues from hip surgeries were collected through the Tissue Donation Program at Northwell Heath and bone marrow aspirates from the Hospital for Special Surgery and the MDS Center at Columbia University. All studies were conducted in accordance with the declaration of Helsinki and under institutional review board (IRB) approval of the New York Blood Center, Northwell Health, the Hospital for Special Surgery and the MDS Center at Columbia University.

Statistical analyses.

Statistical evaluations between different experimental groups were performed using GraphPad Prism 9 (unpaired 2-tailed Student's t-test) and $p<0.05$ was considered to indicate statistical significance.

Other Methods

Additional methods are presented as supplemental materials.

RESULTS

Human erythroid progenitor populations can be divided into distinct subsets

We previously showed that erythroid progenitors capable of forming BFU-E and CFU-E in methylcellulose assays could be isolated based on their CD34/CD36 expression profiles[14]. However, the resulting colonies were heterogeneous in size, indicating that these BFU-E and CFU-E populations were likely mixed populations of erythroid progenitor cells. In addition, we recently demonstrated that two populations of CFU-E, immature and mature CFU-E, could be identified in adult-derived erythroid progenitors using a phenotype of CD71^{hi}CD105^{med} and CD71^{hi}CD105^{hi}, respectively[19]. Thus, the potential of these two markers to resolve heterogeneity was further investigated in erythroid progenitor cell populations. Flow cytometric analyses of the CD34$^+$CD36$^-$, CD34$^+$CD36$^+$, and CD34$^-$CD36$^+$ erythroid progenitor populations (IL3R-GPA-) derived from EPO-differentiated adult CD34$^+$ cells revealed six distinct sub-populations based on CD71/CD105 expression profiles (Fig 1A). Specifically, CD34$^+$CD36$^-$ cells could be divided

into P1 ($CD71^{-}CD105^{-}$) and P2 ($CD71^{+}CD105^{-}$) subpopulations while $CD34^{+}CD36^{+}$ cells were divided into three subpopulations P3 ($CD71^{+}CD105^{-}$), P4 ($CD71^{+}CD105^{low}$) and P5 ($CD71^{+}CD105^{high}$). The vast majority of $CD34^{-}CD36^{+}$ cells were phenotyped as P6 ($CD71^{+}CD105^{high}$).

These six cell populations were sorted and their ability to form colonies in the presence of EPO-alone or in complete medium with SCF, IL3, GM-CSF and EPO was evaluated[20] (Fig 1B and 1C).

EPO-alone media, a condition that only supports CFU-E colony formation[21,22], did not result in the formation of colonies from the P1 population and only a small number of colonies (24±10 per 200 plated cells) from the P2 population. The P3 population generated more colonies than P2 but colony-forming efficiency remained low (72±18 per 200 plated cells). In contrast, the P4 population formed well-hemoglobinized colonies with a significantly higher colony-forming efficiency (144±4 per 200 plated cells; p=0.002). P5 and P6 populations generated typical CFU-E-like colonies (Fig 1B left panel and 1C upper panel).

In complete medium supplemented with SCF, IL3, GM-CSF and EPO, the P1 population generated both erythroid and myeloid colonies, but had a low colony-forming efficiency (4.3±0.2 CFU-GEMM, 50±25 BFU-E and 28±7 CFU-G/M per 200 plated cells). In contrast, the P2 population exhibited a much higher colony-forming efficiency with a predominance of typical multiple-cluster BFU-Es (148±18 B/CFU-E per 200 plated cells). With regards to the transition population, and in accordance with our published findings[19], the P3 population showed a similar colony-forming ability as the P2 population. The P4 population of cells gave rise to a comparable number of erythroid colonies in both EPO-alone and complete media but the colony size was much larger in complete media, implying that this subset is sensitive to SCF-induced proliferation (Fig 1B right panel and 1C bottom panel). As opposed to the P4 population, the sensitivity of the P5 and P6 populations to SCF was decreased, as reflected by a lower augmentation in colony size in complete media. Together, these data demonstrate that the sequential maturation of erythroid progenitors is accompanied by decreased sensitivity to SCF.

SCF is a critical growth factor for erythroid and myeloid progenitors. To better define the differential sensitivity of the six identified erythroid progenitor populations to SCF, the expression levels of CD117/c-Kit, the receptor for SCF ligand, was examined (Fig 1D). All six sub-populations expressed CD117 with lower levels of expression on the P2 and P3 populations. Expression levels increased starting with the P4 population, peaking with the P5 population and subsequently decreasing in the P6 population.

Together, these data indicate that the erythroid progenitor continuum can be immunophenotyped as $CD117^{+}CD71^{+}IL3R^{-}GPA^{-}CD34^{+/-}$ with CD105 expression levels distinguishing the transition from BFU-E to CFU-E.

Validation of the continuum of erythroid progenitors

Following the phenotyping of human erythroid progenitors, we attempted to identify and quantitate the different stages of erythropoiesis. Adult-derived $CD34^+$ cells were differentiated for 5 days in the presence of rEPO and $CD117^+GPA^-$ cells were evaluated (gating out granulocyte-monocyte progenitors (GMPs) and megakaryocyte-committed progenitors (MkPs) as a function of CD45RA and CD41a expression, respectively). Based on the expression levels of CD34 and CD105, the erythroid progenitor compartment ($IL3R^-CD71^+$) could be sub-divided into four distinct populations. We specifically defined $CD34^+CD105^-$ as EP1 (erythroid progenitor 1), $CD34^+CD105^{low}$ as EP2, $CD34^{+/low}CD105^{high}$ as EP3 and $CD34^-CD105^{high}$ as EP4 (Fig 2A).

The morphology of the four sorted erythroid progenitor populations is shown in Fig 2B. The EP1 cell population was consistently smaller than the other three cell populations and showed the highest nuclear/cytoplasmic ratio. An increase in cell size and a decrease in nuclear/cytoplasmic ratio was noted, consistent with the progressive maturation of the progenitor population from EP1 to EP4.

Functional assays on these isolated cell subsets revealed that EP1 is composed predominantly of BFU-E while EP2, EP3 and EP4 represent increasingly mature CFU-E populations with reduced proliferative responsiveness to SCF (Fig 2 C, D and E). These four populations correspond to populations P2 to P6, defined on the basis of CD71/CD105 expression profiles (Fig 1).

To validate our hypothesis that these subsets reflected a continuum of erythroid progenitors, the isolated EPs were cultured to undergo further erythroid differentiation and their differentiation potential monitored (Fig 2F). Following two days of differentiation, flow cytometry analysis showed progressive acquisition of GPA expression ranging from 16% for EP1 to 78% for EP4. More importantly, during two days of culture, EPs progressed along the proposed continuum from EP1 to EP4. Specifically, EP1 progressed into EP2/EP3/EP4, EP2 progressed to EP3/EP4, and EP3 shifted to EP4 (Fig 2F). Finally, we observed that the EP1 population had the highest proliferative capacity with a progressive decrease in the proliferative capacities of EP2, EP3 and EP4 populations, respectively (Fig 2G). Together, these data support the hierarchical progression of erythroid progenitors from an EP1 to EP4 state.

CD34/CD105 expression profiles distinguish the *in vivo* continuum of erythroid progenitors

Based on the *in vitro* analyses presented above, it was of interest to determine whether this profiling strategy could be extended to primary, uncultured human bone marrow samples containing erythroid cells at all stages of erythropoiesis.

Representative flow cytometry plots of positively selected CD117+ cells from bone marrow mononuclear cells are shown in Fig 3A. Following the same strategy used to identify EP1 to EP4 populations, $CD117^+GPA^-CD45RA^-CD41a^-$ cells were subsequently sub-divided into two populations, $IL3R^-CD71^+$ (erythroid lineage) and $IL3R^+CD71^-$ (non-erythroid lineage) subsets. EP1 to EP4 subsets were further gated from the $IL3R^-CD71^+$ compartment based on their CD34 and CD105 profiles (Fig 3A). To exclude any admixture of cells from other

lineages with erythroid progenitors, a lineage cocktail was used to document that all four EP populations were Lin^- (supplemental Fig1A).

To examine the morphology and functionality of these four populations, EP1 to EP4 were FACS sorted. $IL3R^+CD71^-$ cells were also sorted as a control for more primitive progenitors. Although erythroid progenitors in the bone marrow are not morphologically recognizable amongst the highly heterogeneous bone marrow cells, we observed morphological differences between the four groups of sorted erythroid progenitors in terms of cell size and nuclear/cytoplasmic ratio (Fig 3B). Consistent with our data from *in vitro* differentiated $CD34^+$ cells, EP1 cells were the smallest cells and had the highest nuclear/cytoplasmic ratio, similar to the more primitive $IL3R^+CD71^-$ cells. Sequential differentiation from EP1 to EP4 was accompanied by an increase in cell size and a decrease in the nuclear/cytoplasmic ratio. Furthermore, the forward scatter profiles of these cell populations are consistent with noted differences in cell size (Supplemental Fig 1B).

Functional assays on these isolated cells revealed that EP1 is enriched in BFU-Es (100±14 BFU-E per 200 plated cells) in complete medium (Fig 3D), but with fewer well-hemoglobinized CFU-E colonies in conditions of EPO alone (22±13 CFU-E per 200 plated cells) (Fig 3E left panel). As expected, $IL3R^+CD71^-$ cells failed to generate CFU-E colonies in EPO-alone medium but gave rise to more CFU-G and CFU-M as compared to BFU-E in complete medium (28±7 CFU-G/M, 10±5 BFU-E per 200 plated cells). In contrast, while EP2 cells generated a comparable number of erythroid colonies in both types of media (Fig 3E), colonies were much larger in complete media than in EPO-alone media (Fig 3C, D). In contrast, for EP3 and EP4, a similar number of colonies were noted in the two types of media.

Together, these data validate our *in vitro* findings and confirm the existence of four specific and successive stages of erythroid progenitors *in vivo* in human bone marrow. They also identify the critical role of CD105 in distinguishing stages of human erythropoiesis. We find that BFU-E EP1, immature CFU-E EP2, and sequentially mature CFU-Es EP3 and EP4 constitute the continuum of early human erythropoiesis, thereby providing new insights into erythroid progenitor biology.

Decreases in CD105 expression levels distinguish terminally differentiating erythroblasts in human bone marrow

Since CD105 (Endoglin, a member of TGF-β receptor family) is expressed in proerythoblast and basophilic erythroblasts[23,24] (Fig4A), we explored its potential to distinguish distinct stages of terminally differentiating erythroblasts. We found that the expression of CD105 decreased markedly starting with late basophilic erythroblasts; lower levels of expression were detected in polychromatic erythroblasts and little or no expression detected in orthochromatic erythroblasts (Fig 4A).

Representative CD105 and GPA flow cytometry profiles on positively selected $CD71^+$ cells from bone marrow mononuclear cells are shown in Fig 4B. We were able to identify five distinct clusters of cells: $GPA^{low}CD105^{high}$ as proerythroblasts, $GPA^{high}CD105^{high}$ as early basophilic erythroblasts, $GPA^{high}CD105^{int}$ as late basophilic erythroblasts,

GPA^{high}CD105^{low} as polychromatic erythroblasts and GPA^{high}CD105^{-} as orthochromatic erythroblasts. As we have previously shown that the surface expression of α4-integrin and band 3 can be used to distinguish these five distinct stages, we analyzed the overlap of these flow patterns using both strategies (Fig 4 B and C). Morphological Giemsa staining analyses confirmed the purity of the five populations obtained (Fig 4D). Notably, CD105/GPA profiles allowed for a better discrimination than α4-integrin/Band 3 profiles, especially at late stages of the terminal erythroid differentiation.

We then applied this strategy to evaluation of *in vitro* differentiated adult-derived CD34^{+} cells. Proerythroblasts and early basophilic erythroblasts were sorted on day 7 and late basophilic, poly- and orthochromatic erythroblasts were sorted on day 14 of differentiation (Suppl Fig 2A). All five stages of erythroblasts were successfully isolated based on their CD105/GPA profiles and the morphologies of the sorted cells confirmed the five distinct populations (Suppl Fig 2B). Interestingly, similar to our cultured erythroid progenitors, more intracellular vesicles were noted in *in vitro* differentiated proerythroblasts and basophilic erythroblasts, compared to their bone marrow counterparts (Fig 4D and Suppl Fig 2B).

Thus, staining for CD105 in combination with GPA can be used as to resolve all 5 previously described stages of terminal erythropoiesis.

An integrated FACS strategy enables stage-wise detection of human adult erythropoiesis

Having established that cell surface CD105 levels can be used in conjunction with other surface markers to resolve the continuum of erythropoiesis up to reticulocytes, we developed an optimal 10-color flow cytometry strategy using the cell surface markers CD34, CD117, IL3R, CD45RA, CD41a, CD71, CD105, GPA and nucleic acid dye syto16 as well as the cell viability dye 7AAD for a comprehensive analytical strategy to distinguish the nine distinct stages of erythropoiesis in human bone marrow.

For quantitation of erythroid progenitors, GPA^{-} cells were analyzed for expression of CD117 and CD34 and CD117^{+} cells were gated. Based on expression levels of CD45RA and CD41a, the CD45RA^{-}CD41a^{-} cells were gated and expression levels of IL3R and CD71 monitored. Following gating of CD71^{+} cells, the expression levels of CD34 and CD105 were analyzed and four distinct populations of erythroid progenitors, EP1 to EP4 could be quantitated (Fig 5A).

To quantitate terminally differentiated erythroblasts, GPA^{+} cells with high levels of expression of CD71 were analyzed (Fig 5A). CD71^{+}GPA^{+} cells consisted of nucleated erythroblasts (syto16^{+}) and reticulocytes (syto16^{-}). Based on the expression levels of CD105 and GPA, the syto16^{+} erythroblast population could be further divided into five distinct clusters: proerythroblasts, early- and late basophilic erythroblasts, polychromatic erythroblasts and orthochromatic erythroblasts (Fig 5A).

By overlaying these two profiles, nine distinct populations could be easily distinguished, reflecting the continuum of stages of erythropoiesis in human bone marrow (Fig 5B). To further validate this continuum, FACS-purified EPs were cultured and their differentiation was monitored every two days by quantitating the expression of CD105 and GPA. As shown

in Fig 5C, EP1, EP2, EP3 and EP4 differentiated along the CD105/GPA axis as anticipated; EP1 and EP4 subsets required 12 and 8 days respectively to mature into orthochromatic erythroblasts.

We then examined surface expression of erythroid-associated proteins throughout erythropoiesis. As shown in Fig 5D, the expression of CD117 increased during early erythropoiesis and reached a peak at the EP3 stage before decreasing gradually from the EP4 and proerythroblast stage with a subsequent marked reduction at later stages of differentiation. The well-defined erythroid markers, CD71 and CD36 were expressed to varying degrees at all stages of erythroid differentiation. As erythroid progenitors have been identified in the $CD34^{+}CD38^{+}$ compartment[25], and low-level expression of CD45 was previously reported in BFU-E and CFU-E populations[14], we measured their expression levels during the entire course of erythroid development and differentiation. Both CD38 and CD45 were expressed at comparable levels in the EP1 and EP2 populations with decreased levels at the EP3 stage and little or no expression at EP4 stage. Neither of these proteins was expressed in terminally differentiated erythroblasts.

Taken together, the novel flow cytometry-based strategy we have developed enables a comprehensive characterization and quantitation of nine distinct stages of steady-state human adult erythropoiesis. This approach provides a simple, intuitive and comprehensive means to study the dynamic process of normal human erythropoiesis.

The impaired terminal erythroid differentiation in MDS is associated with defective erythroid progenitor differentiation

Ineffective erythropoiesis leading to the sub-optimal production of red cells leads to anemia, a major clinical feature of numerous human red cell disorders including thalassemia and MDS[26,27]. The decreased production of red cells could result from a block at any of the multiple stages of erythropoiesis, Currently, there is no standardized strategy to address this important issue. We therefore explored whether our novel phenotyping strategy could provide new insights into ineffective erythropoiesis.

We assessed erythropoiesis in the bone marrow of 5 patients with MDS using the newly developed strategy. The clinical features and mutational analyses for these 5 patients are shown in Table 1. As shown in Fig 6A, two subjects, MDS-1 and MDS-2 showed comparable terminal erythroid differentiation to that detected in healthy controls. Correspondingly, erythroid progenitor differentiation with reasonable numbers of progenitors at each stage of development were found. In the third subject, MDS-3, there were decreased numbers of mature CFU-E (EP3 and EP4) without a significant effect on terminal differentiation. Significantly impaired terminal erythroid differentiation was detected in subjects MDS-4 and MDS-5, in association with marked decreases in erythroid progenitor populations (Fig 6A).

Quantification of the different subsets of erythroid cells revealed that while the number of erythroblasts increased during successive development stages in healthy controls, decreases in erythroid progenitors resulted in a marked diminuition of terminally differentiated erythroblasts (Fig 6B). These findings imply that defects in erythroid progenitor

differentiation accounts, at least in part, for the impaired terminal erythroid differentiation in MDS. Our findings on a small cohort of MDS subjects begins to provide new insights into our understanding of the underlying mechanisms of ineffective erythropoiesis in MDS and highlights the potential usefulness of this newly established strategy to comprehensively study ineffective erythropoiesis in various human disorders.

Discussion

Erythropoiesis is a complex and tightly regulated process encompassing multiple steps from the hematopoietic stem cell to committed erythroid progenitor cells (BFU-E and CFU-E) and ultimately to mature erythrocytes. This process involves ~ 15 cell divisions and requires a coordinated cell division that is dependent on growth factors, specific niches and physiologic needs. A comprehensive assessment of this process is dependent on the identification of a maximal number of distinct stages, which is a critical prerequisite for the development of a detailed understanding of the underlying regulatory mechanism(s). In contrast to the significant progress made in the phenotypic characterization of myeloid and lymphoid lineages, much less progress has been made in the phenotyping of distinct stages of erythropoiesis. To address this unmet need, we developed an immunophenotyping strategy to monitor human erythropoiesis using a specific set of cell surface markers.

In a previous study, we immunophenotyped IL3R^{-}CD34^{+}CD36^{-}GPA^{-} as BFU-E, IL3R^{-}CD34^{-}CD36^{+}GPA^{-} as CFU-E, and CD34^{+}CD36^{+} progenitors as a mixture containing BFU-E and CFU-E[14,17]. However, while it appeared that these populations represented distinct stages of erythroid progenitors, the isolated cell populations were functionally heterogeneous[18,19], indicating that further characterization was needed. Based on the expression of CD36 and CD105, in the previously defined MEP population (Lin-CD34^{+}CD38^{+}CD45RA^{-}IL3R^{-})[25], Iskander and colleagues identified Early Erythroid Progenitor (EEP) and Late Erythroid Progenitor (LEP) populations, generating BFU-E and CFU-E colonies, respectively[15]. Also from this population of Lin-CD34^{+}CD38^{+}CD45RA^{-}IL3R^{-} MEPS, Morris and colleagues documented that CD71^{+} CD105^{-} MEPs primarily generated large erythroid colonies while CD71$^{int/+}$ CD105^{+} MEPs gave rise mostly to CFU-E colonies[16]. Both studies focused on the CD34^{+} cell compartment indicating that CD105 could serve as a key marker to distinguish CFU-E from BFU-E.

By integrating CD71 and CD105 into our previously established surface marker phenotyping evaluation, we delineated the heterogeneity of previously defined populations of erythroid progenitors and identified four successive stages of erythroid progenitors. The four populations from EP1 to EP4 constitute continuum of committed erythroid progenitors and enable the stage-specificity of early erythropoiesis to be refined. Notably, the lower erythroid colony-forming efficiency of EP1, particularly in cells isolated from primary bone marrow cells, suggest the presence of a small proportion of bi-potential MEP in the EP1 population. Recent studies have indicated that CD38 and MPL can be used to identify rare MEPs[28–30] and as such further studies are warranted to study the specification of MEP to erythroid-committed progenitors, especially EP1, in the bone marrow.

Furthermore, we found that CD105 can be used to study terminal erythroid differentiation. In a previous study, we documented the importance of that the surface markers, GPA, α4-integrin and Band3 markers to distinguish between five distinct stages of terminal erythroid differentiation[12]. In the present study, we find that GPA and CD105 provide a more precise discrimination of these five distinct development stages. This finding therefore enables us to resolve the full continuum of erythropoiesis using one comprehensive set of markers.

As the availability of human bone marrow samples is limited, *in vitro* culture of $CD34^+$ HSPCs has been widely used as a model of human normal and disordered erythropoiesis[31–36]. However, differences between *in vitro* models and "true" *in vivo* erythropoiesis in human bone marrow exist. While the functional features of erythroid progenitors and erythroblasts are largely similar between these two systems, some differences exist[12]. Based on cytospin images of isolated cells at equivalent stages of development as a function of GPA/CD105 profiles, we detected a greater abundance of larger sized vesicles from the EP1 subset to polychromatic erythroblast stages in *in vitro* differentiated as compared to *in vivo* BM-differentiated subsets. These vesicles appear to be lipid droplets (our unpublished data) and our data suggest that they are likely the result of metabolic stress response occurring during *in vitro* differentiation.

Our study enables a precise characterization of specific stages of human erythropoiesis, promoting the study of specific erythroid defects in disorders with aberrant or ineffective erythropoiesis. In our cohort of MDS patients, we were able to identify defects at different stages of erythroid progenitor development. Admittedly, this is a small cohort but we believe that our novel method will be applicable to the study of MDS patients as well as patients with other anemias. We expect that future studies will advance our understanding of the mechanisms underlying these disorders and promote evaluation of specific therapies, including corticosteroids and immunomodulatory agents, in rescuing erythropoiesis in these patients.

In summary, we have developed an efficient and comprehensive immunophenotyping strategy to characterize the multiple stages of human erythropoiesis. We anticipate that this technique will serve as a valuable new tool, promoting our understanding of normal and disordered human erythropoiesis.

Supplementary Material

Refer to Web version on PubMed Central for supplementary material.

Acknowledgements

This research was supported in part by NIH grants DK32094 (N.M, P.G.G, S.K), HL144436 and HL152099 (L.B).

References

1. Palis JPrimitive and definitive erythropoiesis in mammals. Front Physiol. 2014;5:3. [PubMed: 24478716]
2. Loken M, Shah V, Dattilio K, Civin C. Flow cytometric analysis of human bone marrow. II. Normal B lymphocyte development. Blood. 1987;70(5):1316–1324. [PubMed: 3117132]

3. Terstappen LWMM, Safford M, Loken MR. Flow cytometric analyisis of human bone marrow III. Neutrophil maturation. Leukemia. 1990;4(9):657–663. [PubMed: 2395385]
4. Terstappen LWMM, Loken MR. Myeloid cell differentia tion in normal bone marrow and acute myeloid leukemia assessed by multi-dimensional flow cytometry. Anal cullular Pathol. 1990;2:229–240.
5. Robinson J, Sieff C, Delia D, Edwards PA, Greaves M. Expression of cell-surface HLA-DR, HLA-ABC and glycophorin during erythroid differentiation. Nature. 1981;289(5793):68–71. [PubMed: 6161308]
6. Sieff C, Bicknell D, Caine G, Robinson J, Lam G, Greaves MF. Changes in cell surface antigen expression during hemopoietic differentiation. Blood. 1982;60(3):703–713. [PubMed: 6286014]
7. Loken MR, Shah VO, Dattilio KL, Civin CI. Flow cytometric analysis of human bone marrow: I. Normal erythroid development. Blood. 1987;69(1):255–263. [PubMed: 2947644]
8. Okumura N, Tsuji K, Nakahata T. Changes in Cell Surface Antigen Expressions During Proliferation and Differentiation of Human Erythroid Progenitors. Blood. 1992.
9. van Lochem EG, van der Velden VHJ, Wind HK, te Marvelde JG, Westerdaal NAC, van Dongen JJM. Immunophenotypic differentiation patterns of normal hematopoiesis in human bone marrow: Reference patterns for age-related changes and disease-induced shifts. Cytometry. 2004;60B(1):1–13.
10. Terszowski G, Waskow C, Conradt P, et al.Prospective isolation and global gene expression analysis of the erythrocyte colony-forming unit (CFU-E). Blood. 2005;105(5):1937–1945. [PubMed: 15522951]
11. Pronk CJH, Rossi DJ, Månsson R, et al.Elucidation of the Phenotypic, Functional, and Molecular Topography of a Myeloerythroid Progenitor Cell Hierarchy. Cell Stem Cell. 2007;1(4):428–442. [PubMed: 18371379]
12. Hu J, Liu J, Xue F, et al.Isolation and functional characterization of human erythroblasts at distinct stages: implications for understanding of normal and disordered erythropoiesis in vivo. Blood. 2013;121(16):3246–3253. [PubMed: 23422750]
13. Wangen JR, Eidenschink Brodersen L, Stolk TT, Wells DA, Loken MR. Assessment of normal erythropoiesis by flow cytometry: Important considerations for specimen preparation. Int J Lab Hematol. 2014;36(2):184–196. [PubMed: 24118926]
14. Li J, Hale J, Bhagia P, et al.Isolation and transcriptome analyses of human erythroid progenitors: BFU-E and CFU-E. Blood. 2014;124(24):3636–3645. [PubMed: 25339359]
15. Iskander D, Psaila B, Gerrard G, et al.Elucidation of the EP defect in Diamond-Blackfan anemia by characterization and prospective isolation of human EPs. Blood. 2015;125(16):2553–2557. [PubMed: 25755292]
16. Mori Y, Chen JY, Pluvinage JV., Seita J, Weissman IL. Prospective isolation of human erythroid lineage-committed progenitors. Proc Natl Acad Sci. 2015;112(31):9638–9643. [PubMed: 26195758]
17. Yan H, Hale J, Jaffray J, et al.Developmental Differences Between Neonatal and Adult Human Erythropoiesis. Am J Hematol. 2018;93:494–503. [PubMed: 29274096]
18. Dulmovits BM, Hom J, Narla A, et al.Characterization, regulation and targeting of erythroid progenitors in normal and disordered human erythropoiesis. Curr Opin Hematol. 2017;24(3):159–166. [PubMed: 28099275]
19. Ashley RJ, Yan H, Narla A, Blanc L. Steroid resistance in Diamond Blackfan anemia associates with p57 Kip2 dysregulation in erythroid progenitors Graphical abstract The Journal of Clinical Investigation. J Clin Invest. 2020;130(4):2097–2110. [PubMed: 31961825]
20. Dover GJ, Chan T, Sieber F. Fetal hemoglobin production in cultures of primitive and mature human erythroid progenitors: differentiation affects the quantity of fetal hemoglobin produced per fetal-hemoglobin-containing cell. Blood. 1983;61(6):1242–1246. [PubMed: 6188507]
21. Stephenson JR, Axelrad AA, Mcleod DL, Shreeve MM. Induction of Colonies of Hemoglobin-Synthesizing Cells by Erythropoietin In Vitro. PNAS. 1971;68(7):1542–1546. [PubMed: 4104431]
22. Dai CH, Krantz SB, Zsebo KM. Human Burst-Forming Units-Erythroid Need Direct Interaction With Stem Cell Factor for Further Development. Blood. 1991;78(10):2493–2497. [PubMed: 1726703]

23. Bühring HJ, Müller CA, Letarte M, et al.Endoglin is expressed on a subpopulation of immature erythroid cells of normal human bone marrow. Leukemia. 1991;5(10):841–847. [PubMed: 1961019]
24. Rokhlin OW, Cohen MB, Kubagawa H, Letarte M, Cooper MD. Differential expression of endoglin on fetal and adult hematopoietic cells in human bone marrow. J Immunol. 1995;154(9):4456–4465. [PubMed: 7722302]
25. Manz MG, Miyamoto T, Akashi K, Weissman IL. Prospective isolation of human clonogenic common myeloid progenitors. Proc Natl Acad Sci U S A. 2002;99(18):11872–11877. [PubMed: 12193648]
26. Ali AM, Huang Y, Pinheiro RF, et al.Severely impaired terminal erythroid differentiation as an independent prognostic marker in myelodysplastic syndromes. Blood Adv. 2018;2(12):1393–1402. [PubMed: 29903708]
27. Taher AT, Musallam KM, Cappellini MD. β-Thalassemias. Longo DL, ed. N Engl J Med. 2021;384(8):727–743. [PubMed: 33626255]
28. Sanada C, Xavier-Ferrucio J, Lu Y-C, et al.Adult human megakaryocyte-erythroid progenitors are in the CD34 + CD38 mid fraction. Blood. 2016;128:923–933. [PubMed: 27268089]
29. Xavier-Ferrucio J, Krause DS. Concise Review: Bipotent Megakaryocytic-Erythroid Progenitors: Concepts and Controversies. Stem Cells. 2018;36(8):1138–1145. [PubMed: 29658164]
30. Lu Y-C, Sanada C, Xavier-Ferrucio J, et al.The Molecular Signature of Megakaryocyte-Erythroid Progenitors Reveals a Role for the Cell Cycle in Fate Specification HHS Public Access. Cell Rep. 2018;25(8):2083–2093. [PubMed: 30463007]
31. Fibach E, Manor D, Oppenheim A, Rachmilewitz EA. Proliferation and Maturation of Human Erythroid Progenitors in Liquid Culture. Blood. 1989;73(1):100–103. [PubMed: 2910352]
32. Panzenbö B, Bartunek P, Mapara MY, Zenke M. Growth and Differentiation of Human Stem Cell Factor/Erythropoietin-Dependent Erythroid Progenitor Cells In Vitro. Blood. 1998;92(10):3658–3668. [PubMed: 9808559]
33. Giarratana M-C, Kobari L, Lapillonne H, et al.Ex vivo generation of fully mature human red blood cells from hematopoietic stem cells. Nat Biotechnol. 2005;23(1):69–74. [PubMed: 15619619]
34. Bouhassira EE. Concise Review: Production of Cultured Red Blood Cells from Stem Cells. Stem Cells Transl Med. 2012;1(12):927–933. [PubMed: 23283554]
35. Fibach EErythropoiesis In Vitro—A Research and Therapeutic Tool in Thalassemia. J Clin Med. 2019;8(12):2124.
36. Deleschaux C, Moras M, Lefevre SD, Ostuni MA. An overview of different strategies to recreate the physiological environment in experimental erythropoiesis. Int J Mol Sci. 2020;21(15):1–15.

KEY POINTS

- Erythropoiesis in primary human bone marrow can be resolved into a continuum of 9 distinct stages.
- Resolving the human erythropoietic continuum has mechanistic implications for our understanding of ineffective erythropoiesis.

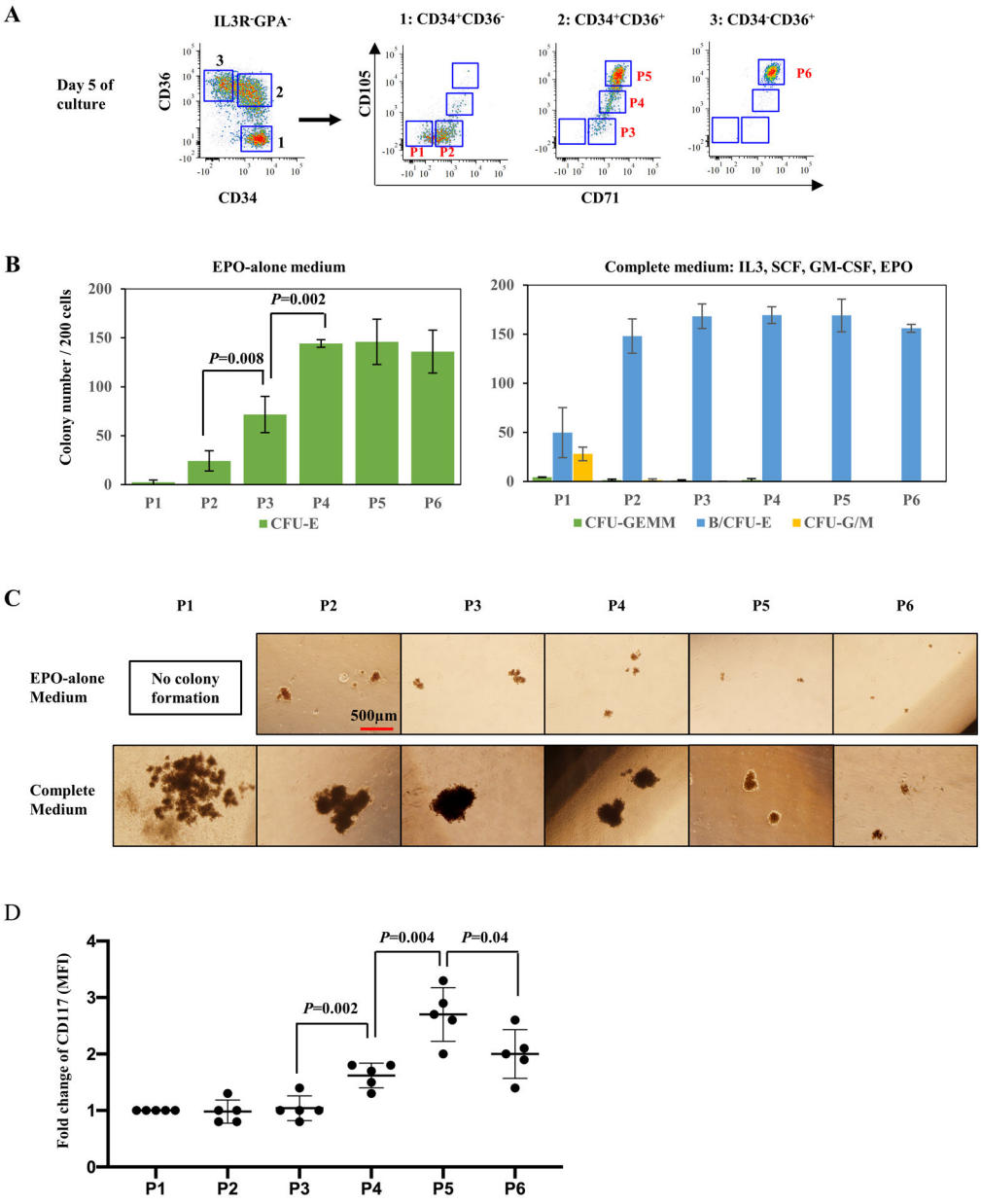

Figure 1. Human erythroid progenitor populations can be divided into distinct subsets.

(A) Representative FACS plots illustrating expression of CD71 and CD105 in previously defined erythroid progenitor populations $CD34^{+}CD36^{-}$, $CD34^{+}CD36^{+}$ and $CD34^{-}CD36^{+}$. Based on their expression, six subsets including P1, P2, P3, P4, P5 and P6, were gated and sorted for colony forming assay. (B) Number of colonies generated from 200 FACS-sorted cells of P1-P6, separately, in EPO-alone medium (upper panel) and complete medium (lower panel). Error bars indicate standard deviation (SD) of the mean (n=4). (C) Representative images of colonies generated by P1 to P6 cells, in EPO-alone and complete medium. The photos were taken under an inverted microscope at ×4 magnification, scale bar=500μm. (D) CD117 expression on surface of P1 to P6 cells. Error bars indicate standard deviation (SD) of the mean (n=5).

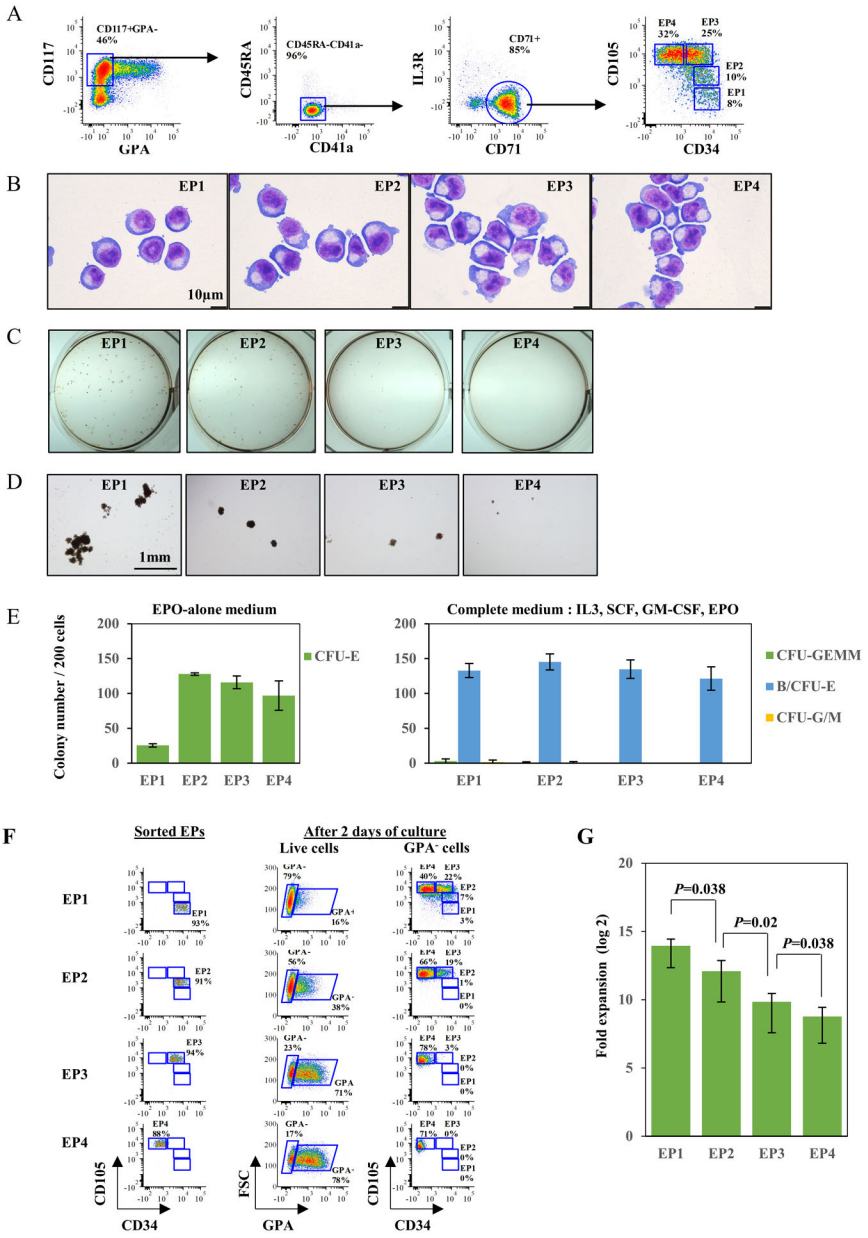

Figure 2. Validation of the continuum of erythroid progenitors

(A) Representative FACS plots for definition of erythroid progenitors from *in vitro* culture of human $CD34^+$ cells, on day 5 of differentiation. (B) Representative cytospin images of sorted $IL3R^+CD71^-$, EP1, EP2, EP3 and EP4 cells from *in vitro* culture of human $CD34^+$ cells. The cells were sorted on day 5 of differentiation. The images were captured under Leica DM2000 microscope at ×100 magnification, scale bar=10μm. (C) Representative images of colonies generated by sorted $IL3R^+CD71^-$, EP1, EP2, EP3 and EP4 cells from *in vitro* culture of human $CD34^+$ cells, in complete medium. The photos were taken using a Nikon D3500 camera. (D) Representative images of colonies generated by sorted $IL3R^+CD71^-$, EP1, EP2, EP3 and EP4 cells from *in vitro* culture of human $CD34^+$ cells, in complete medium. The photos were taken under an inverted microscope at ×4 magnification,

scale bar=1mm. (E) Quantitative analysis of colony forming ability of sorted IL3R^{+}CD71^{-}, EP1, EP2, EP3 and EP4 cells from *in vitro* culture of human CD34^{+} cells. The data are from three independent experiments. (F) Representative FACS plots for sorting purity of EP1, EP2, EP3 and EP4 (left panel) and their differentiation progress after two days of culture (right panel). (G) Number of cell divisions of EP1 to EP4 by the end of differentiation. The numbers were calculated based on final erythroid yield of EP1 to EP4 under same culture conditions. The data are from three independent experiments.

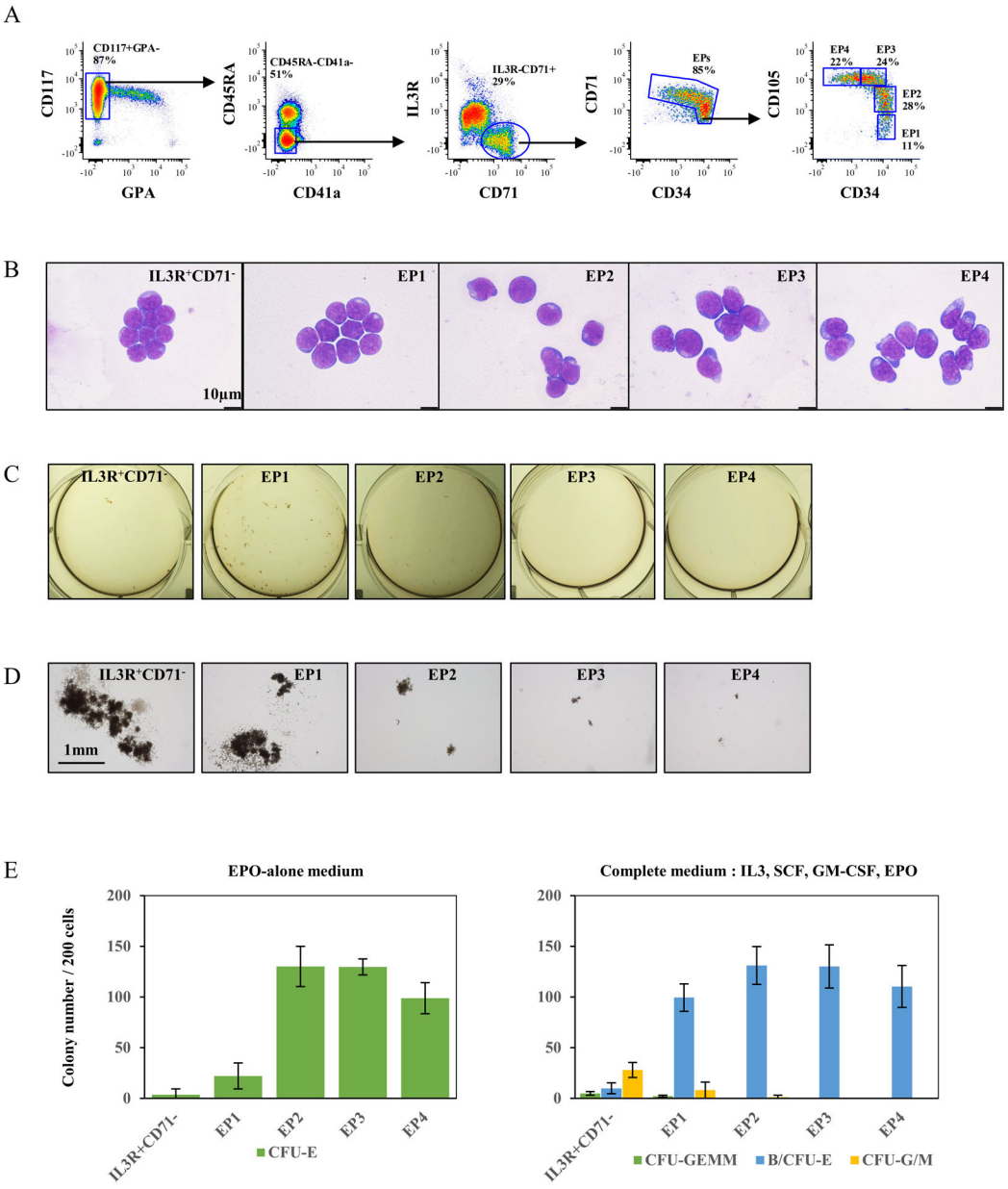

Figure 3. CD34/CD105 expression profiles distinguish the *in vivo* continuum of erythroid progenitors

(A) Representative FACS plots illustrating strategy for definition of erythroid progenitors using enriched $CD117^+$ cells from primary bone marrow. The gates of EP1 to EP4 were made based on expression of CD34 and CD105. (B) Representative cytospin images of sorted $IL3R^+CD71^-$, EP1, EP2, EP3 and EP4 cells from primary bone marrow. The images were captured under Leica DM2000 microscope at ×100 magnification, scale bar=10μm. (C) Representative images of colonies generated by sorted $IL3R^+CD71^-$, EP1, EP2, EP3 and EP4 cells, in complete medium. The photos were taken using a Nikon D3500 camera. (D) Representative images of colonies generated by sorted $IL3R^+CD71^-$, EP1, EP2, EP3 and EP4 cells, in complete medium. The photos were taken under an inverted microscope at ×4

magnification, scale bar=1mm. (E) Quantitative analysis of colony forming ability of sorted IL3R^{+}CD71^{-}, EP1, EP2, EP3 and EP4 cells from six independent experiments.

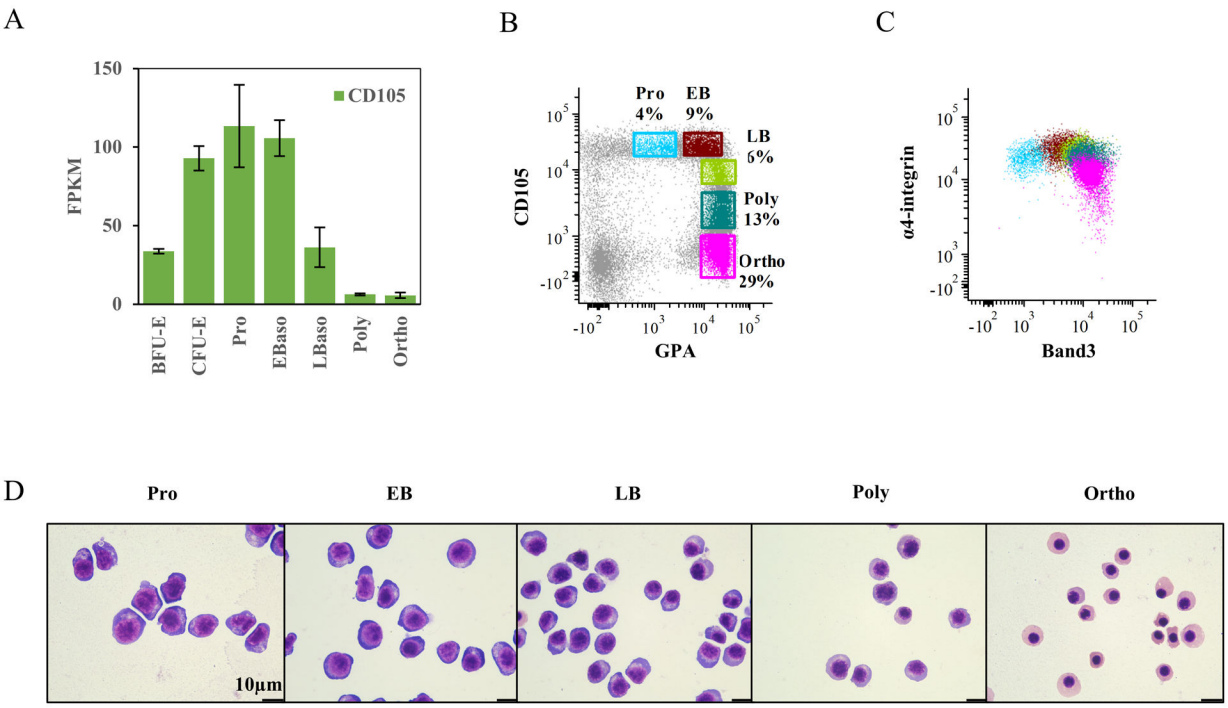

Figure 4. Decreases in CD105 expression levels distinguish terminally differentiating erythroblasts in human bone marrow.

(A) Relative mRNA expression of CD105 at distinct stages of erythroid differentiation. The data are from RNA-seq on 3 biological replicates. (B) Representative FACS plots for definition of erythroblasts at distinct stages. The gates were made based on expression of CD105 and GPA. (C) Dot plot overlay of gated erythroblast populations showing their expression of α4-integrin and Band3. The color of each population sources from the gating plot (B). (D) Representative cytospin images of sorted erythroblasts at distinct stages from primary bone marrow. The images were captured under Leica DM2000 microscope at ×100 magnification, scale bar=10μm.

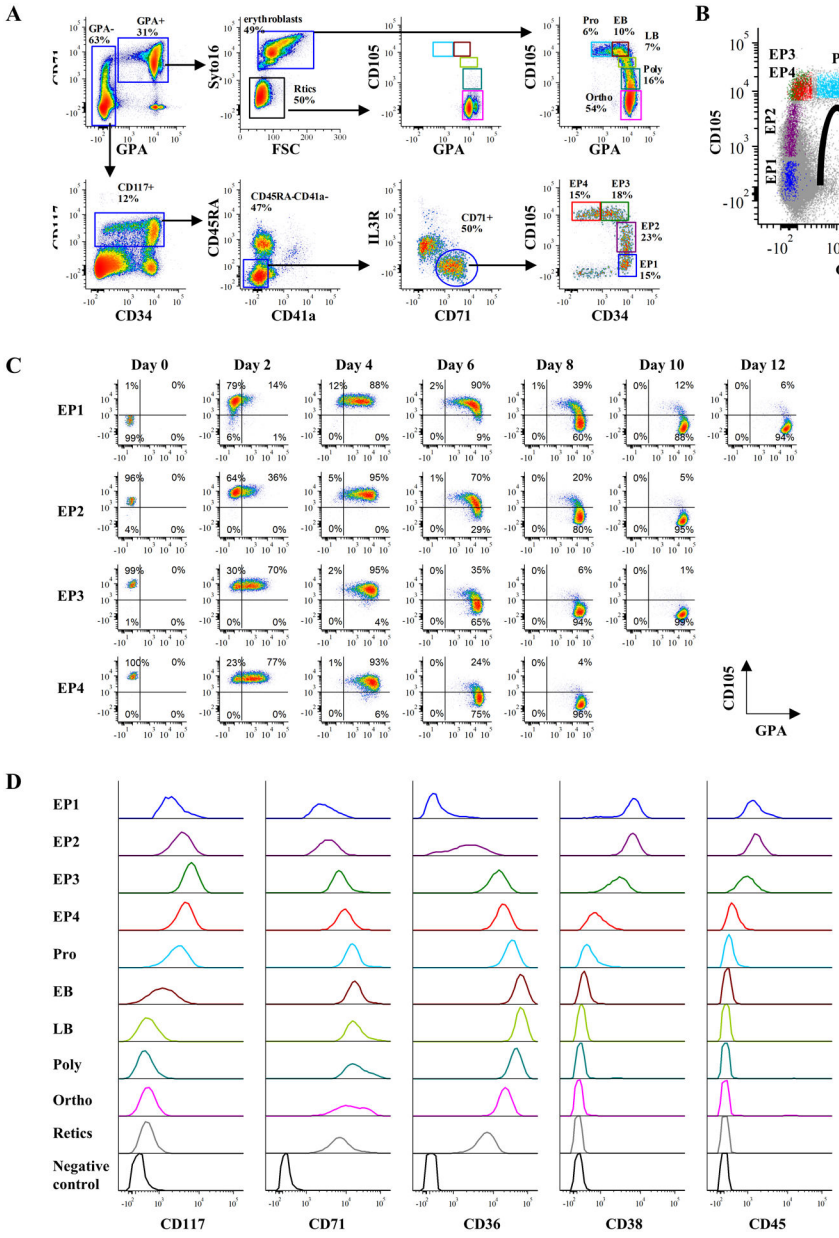

Figure 5. An integrated FACS strategy enables stage-wise detection of human adult erythropoiesis.

(A) Representative FACS plots illustrating an integrated gating strategy for human erythroid continuum from BFU-E to reticulocytes from primary human bone marrow. (B) Dot plot overlay of gated erythroid progenitor and erythroblast populations showing their expression of CD105 and GPA. The color of each population sources from the gating plot (A) and the curved arrow indicates the erythroid differentiation trajectory. (C) Representative FACS plots showing sequential maturation of sorted EP1, EP2, EP3 and EP4 in culture along the indicated trajectory in (B). (D) Representative histograms of erythroid-associated genes expression (CD117, CD71, CD36, CD38 and CD45) in primary human bone marrow cells at distinct erythroid differentiation stage.

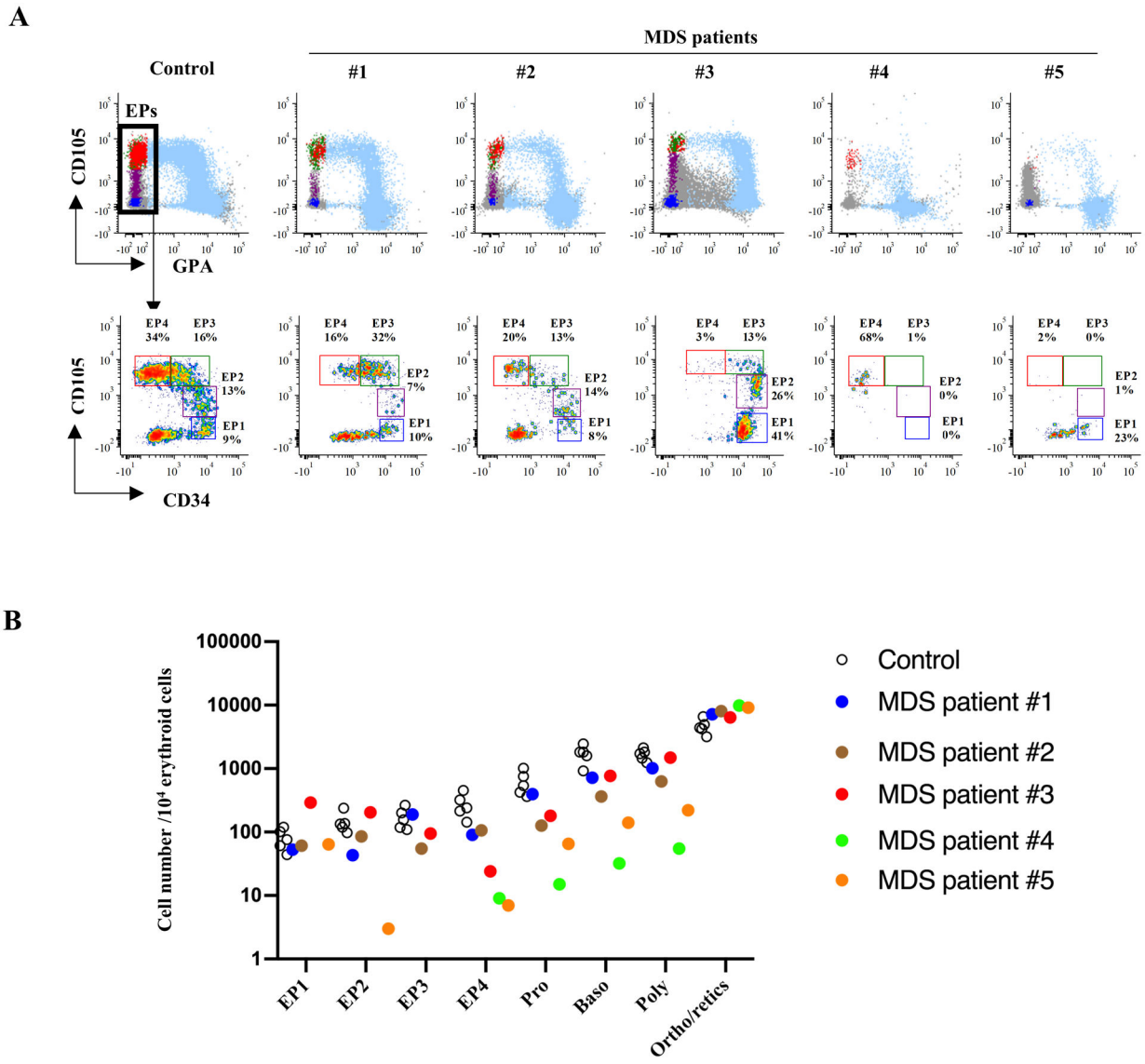

Figure 6. The impaired terminal erythroid differentiation in MDS is associated with defective erythroid progenitor differentiation.

(A) The FACS plots showing erythroid continuum in MDS. The upper panel shows CD105/GPA overlay of erythroid populations, and the lower panel shows further analysis on erythroid progenitor differentiation. (B) Quantification of erythroid progenitors and erythroblasts showing decreased EPs in MDS patients with impaired terminal erythroid differentiation. The Y-axis indicates the cell number of each population in 10^4 erythroid cells. The black circles are healthy controls and the colored dots represent the different MDS samples. Each color corresponds to a specific MDS sample.

Table 1.

The clinical features and mutational analyses of MDS patients.

Patient No.	Age	Gender	Diagnosis	Transfusion	Somatic mutations in genes	Aspirate ME ratio	Hg (g/dL)	Hematocrit (%)	Risk Group
1	68	M	MDS-RS-MLD	None	SF3B1; SRSF2	4:1	9.7	30.3	Intermediate
2	72	M	MDS-RS-MLD	Transfusion dependent	SF3B1; DNMT3A; TET2; NF1	3:1	8.9	25.6	High
3	80	M	MDS/MPN-Unclassifiable or CMML-2	None	SRSF2; STAG2; JAK2; IDH2; RUNX1	7:1	8.7	28.8	Intermediate
4	67	M	MDS-EB1	None	U2AF1; BCOR; STAG2; NRAS	1:1	7.5	24.5	Intermediate
5	62	F	MDS-EB1	None	SF3B1	2:1	8	24.5	High